Generation of radially polarized beams based on thermal analysis of a working cavity

Guangyuan He, Jing Guo, Biao Wang, and Zhongxing Jiao*

State Key Laboratory of Optoelectronic Materials and Technologies, School of Physics and Engineering, Sun Yat-sen University, Guangzhou 510275, China
** jiaozhx@mail.sysu.edu.cn*

Abstract: The laser oscillation and polarization behavior of a side-pumped Nd:YAG laser are studied theoretically and experimentally by a thermal model for a working cavity. We use this model along with the Magni method, which gives a new stability diagram, to show important characteristics of the resonator. High-power radially and azimuthally polarized laser beams are obtained with a Nd:YAG module in a plano-plano cavity. Special regions and thermal hysteresis loops are observed in the experiments, which are concordant with the theoretical predictions.

OCIS codes: (140.3410) Laser resonators; (140.3530) Lasers, neodymium; (140.6810) Thermal effects; (260.5430) Polarization.

References and links

1. Q. Zhan and J. R. Leger, "Focus shaping using cylindrical vector beams," Opt. Express **10**(7), 324–331 (2002).
2. Y. Liu, D. Cline, and P. He, "Vacuum laser acceleration using a radially polarized CO2 laser beam," Nucl. Instrum. Methods Phys. Res. A **424**(2-3), 296–303 (1999).
3. H. Kawauchi, K. Yonezawa, Y. Kozawa, and S. Sato, "Calculation of optical trapping forces on a dielectric sphere in the ray optics regime produced by a radially polarized laser beam," Opt. Lett. **32**(13), 1839–1841 (2007).
4. M. Meier, V. Romano, and T. Feurer, "Material processing with pulsed radially and azimuthally polarized laser radiation," Appl. Phys., A Mater. Sci. Process. **86**(3), 329–334 (2007).
5. L. Novotny, M. R. Beversluis, K. S. Youngworth, and T. G. Brown, "Longitudinal field modes probed by single molecules," Phys. Rev. Lett. **86**(23), 5251–5254 (2001).
6. K. Youngworth and T. Brown, "Focusing of high numerical aperture cylindrical-vector beams," Opt. Express **7**(2), 77–87 (2000).
7. V. G. Niziev and A. V. Nesterov, "Influence of beam polarization on laser cutting efficiency," J. Phys. D **32**(13), 1455–1461 (1999).
8. A. V. Nesterov, V. G. Niziev, and V. P. Yakunin, "Generation of high-power radially polarized beam," J. Phys. D **32**(22), 2871–2875 (1999).
9. R. Oron, S. Blit, N. Davidson, A. A. Friesem, Z. Bomzon, and E. Hasman, "The formation of laser beams with pure azimuthal or radial polarization," Appl. Phys. Lett. **77**(21), 3322–3324 (2000).
10. Y. Kozawa, S. Sato, T. Sato, Y. Inoue, Y. Ohtera, and S. Kawakami, "Cylindrical vector laser beam generated by the use of a photonic crystal mirror," Appl. Phys. Express **1**, 022008 (2008).
11. S. C. Tidwell, D. H. Ford, and W. D. Kimura, "Generating radially polarized beams interferometrically," Appl. Opt. **29**(15), 2234–2239 (1990).
12. T. Moser, H. Glur, V. Romano, F. Pigeon, O. Parriaux, M. A. Ahmed, and T. Graf, "Polarization-selective grating mirrors used in the generation of radial polarization," Appl. Phys. B **80**(6), 707–713 (2005).
13. I. Moshe, S. Jackel, and A. Meir, "Production of radially or azimuthally polarized beams in solid-state lasers and the elimination of thermally induced birefringence effects," Opt. Lett. **28**(10), 807–809 (2003).
14. G. Machavariani, Y. Lumer, I. Moshe, A. Meir, S. Jackel, and N. Davidson, "Birefringence-induced bifocusing for selection of radially or azimuthally polarized laser modes," Appl. Opt. **46**(16), 3304–3310 (2007).
15. A. Ito, Y. Kozawa, and S. Sato, "Selective oscillation of radially and azimuthally polarized laser beam induced by thermal birefringence and lensing," J. Opt. Soc. Am. B **26**(4), 708–712 (2009).
16. W. Koechner, *Solid-state laser engineering* (Springer Verlag, 2006).
17. N. Hodgson, C. Rahlff, and H. Weber, "Dependence of the refractive power of Nd: YAG rods on the intracavity intensity," Opt. Laser Technol. **25**(3), 179–185 (1993).
18. C. C. Cheng, T. L. Huang, S. H. Chang, H. S. Tsai, and H. P. Liu, "Observation of Less Heat Generation and Investigation of Its Effect on the Stability Range of a Nd: YAG Laser," Jpn. J. Appl. Phys. **39**(Part 1, No. 6A), 3419–3421 (2000).
19. V. Magni, "Resonators for solid-state lasers with large-volume fundamental mode and high alignment stability," Appl. Opt. **25**(1), 107–117 (1986).

#151807 - $15.00 USD Received 27 Jul 2011; revised 20 Aug 2011; accepted 22 Aug 2011; published 2 Sep 2011

1. Introduction

Radially and azimuthally polarized laser beams have drawn more and more attention in recent years. Due to the unique properties, radially and azimuthally polarized laser beams can be used in many research fields: focus shaping technique [1], vacuum laser acceleration [2], optical trapping [3], and material processing [4], etc [5–7].

There are various methods to produce radially and azimuthally polarized laser beams [8–12]. A simple and effective way to produce these beams is using the thermal bipolar lensing effect in uniformly pumped isotropic solid-state rods [13–15]. The mode selection in this method is based on the fact that radially and azimuthally polarized beams focus differently in the rods. The cavities of this method are easy to align, without special optical elements. Also it can get high power and good beam quality. According to this idea, I. Moshe *et al.* developed a method of producing radially or azimuthally polarized beams with an aperture inside the cavity [13]. G. Machavariani *et al.* developed a round-trip matrix diagonalization method for a quantitative description of the selection of radially or azimuthally polarized beams in a resonator with a mode selective aperture [14]. A. Ito *et al.* obtained radially or azimuthally polarized beams without the help of any additional optical components only by changing the cavity length [15].

The polarization selectivity of the resonator has been explained by a stability diagram of a laser cavity [14,15]. However, the thermal bipolar lensing effect was experimentally obtained in a non-lasing laser rod. This is not an accurate method because the thermal heat decreases due to laser cooling in a working cavity [16–18]. Therefore the refractive power of the thermal lens is a function of the internal intensity of the cavity. For the purpose to predict the characteristics of the cavity more exactly, it is necessary to survey the behavior of a working cavity.

The thermal model for a working cavity with a flashlamp-pumped Nd:YAG rod has been developed by N. Hodgson *et al.* [17]. However, a formal and comprehensive application to the resonator analysis is lacking. In this research, we present a modified thermal model that, along with the Magni method, provides an analytical tool for describing the oscillation and polarization behavior of a cw-pumped working cavity. The dynamic behaviors of the output power in the processes of increasing and decreasing the pump power are discussed in details. The appropriate regions for producing high-power and steady radially or azimuthally polarized beams are proposed. The model also predicts that special regions and thermal hysteresis loops will appear around the edges of the stable zones. The experimental results, obtained with a cw diode side-pumped Nd:YAG laser, confirm the theoretical predictions and tens of watts radially or azimuthally polarized laser beams are obtained.

2. Thermal lensing effect of the laser material in a working cavity

Temperature gradients of a laser rod caused by a heat flow to the cooled outer periphery can lead to the thermal lensing effect and the thermal induced birefringence effect, which will result in bipolar lensing. By ignoring the end effect of a laser rod, the refractive power (inverse of the focal length) of the thermal lens can be written as [16]

$$D_{r,\phi} = \frac{P_h}{KA}\left(\frac{1}{2}\frac{dn}{dT} + \alpha C_{r,\phi} n_0^3\right), \tag{1}$$

where

P_h is the thermal heat dissipated in the rod,

A is the rod cross-sectional area,

K is the thermal conductivity,

dn/dT is the change of refractive index with temperature,

n_0 is the refractive index of the rod,

#151807 - $15.00 USD Received 27 Jul 2011; revised 20 Aug 2011; accepted 22 Aug 2011; published 2 Sep 2011

α is the thermal coefficient of expansion,

C_r, C_φ are the functions of the elasto-optical coefficients of the laser rod, with different values for radially and azimuthally polarized beams.

The refractive power has often been simply assumed to be a linear function of the pump power. In fact, it is also a function of the internal intensity of the cavity. A thermal model for a working cavity with a flashlamp-pumped Nd:YAG rod has been developed by N. Hodgson *et al.* [17]. Here, we change the pumping condition to continuous laser diodes pumping, and rewrite the expression of P_h as

$$P_h = \chi \eta_{LD} P_{LD} - L P_{\text{int}}, \tag{2}$$

where

$$L = -\frac{\tau_f}{\tau_{nr}} \ln\left(R^{1/2} V_S V_A\right) - 1 + V_A, \tag{3}$$

χ is the thermal load parameter without laser oscillation,

P_{int} is the internal power of the cavity,

P_{LD} is the pump power of the laser diode,

η_{LD} is the ratio of the stored energy to the pumping energy of the laser diodes,

R is the reflectivity of the output coupler,

V_s is the loss factor per transit due to scattering (1-loss),

V_A is the loss factor per transit due to absorption,

τ_f is the fluorescence lifetime from the upper level to the ground state,

τ_{nr} is the non-radiative decay lifetime of the upper level.

Equation (2) implies a reduction of the thermal load under a lasing condition, and the reduction depends on the internal power. The coefficient L introduced here in Eq. (3) describes the efficiency of the laser cooling in the laser rod. It is relevant to the property of the laser rod (τ_f, τ_{nr}, V_A) and the cavity character (R, V_s). A laser operating on the radial polarization mode, azimuthal polarization mode or multimode with the same mode volume in a simple cavity without additional elements may achieve the same L value due to the invariance property of the laser rod and the cavity.

The internal power and the output power of a continuous wave laser are [16]

$$P_{\text{int}} = -\frac{\eta_{LD}\eta_B}{\ln\left(R^{1/2} V_S V_A\right)}\left(P_{LD} - P_{th}\right), \tag{4}$$

$$P_{out} = \frac{1-R}{1+R} P_{int}, \tag{5}$$

where

$$P_{th} = -\ln\left(R^{1/2} V_S V_A\right) \cdot \frac{A h\nu}{\eta_{LD}\eta_B \sigma \tau_f}, \tag{6}$$

η_{B} is the beam overlap efficiency, σ is the stimulated emission cross section, $h\nu$ is the photon energy of the laser.

#151807 - $15.00 USD Received 27 Jul 2011; revised 20 Aug 2011; accepted 22 Aug 2011; published 2 Sep 2011

By inserting Eqs. (3) (4) (6) into Eq. (2), we can obtain the expression of P_h under the lasing condition. Combining with P_h in the non-lasing case, the general expression of P_h can be written as

$$P_h = \begin{cases} \chi \eta_{LD} P_{LD} & (\text{non-lasing}) \\ \left\{ \chi - \eta_B \left[\dfrac{\tau_f}{\tau_{nr}} + \left(1 - V_A\right) \Big/ \ln\left(R^{1/2} V_S V_A\right) \right] \right\} \eta_{LD} P_{LD} + \dfrac{ALh\nu}{\sigma \tau_f} & (\text{lasing}) \end{cases}. \quad (7)$$

The term in the brace of Eq. (7) can be considered as an effective thermal load parameter (χ_{eff}) under the lasing condition. It is noted that χ_{eff} must be less than χ.

Combining Eq. (1) with Eq. (7), the refractive power of the laser rod for a working cavity under a certain pump power can be calculated. Using the resonator analysis method developed by Magni *et al.* [19] and the thermal model described here, we can show important characteristics of the resonator. Also, the output power performance can be analyzed by Eq. (5). The analysis will be shown in the next section. In our simulations, the physical parameters of the Nd:YAG laser rod in Eqs. (1)-(7) can be found in ref [16]. and [17]. The other parameters of the cavity will be described later.

3. Laser performance in the processes of increasing and decreasing the pump power

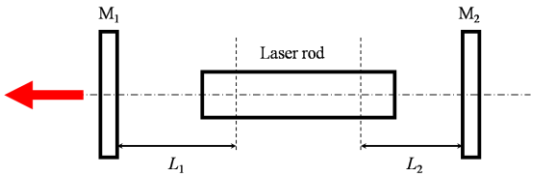

Fig. 1. Schematic of a laser cavity.

Figure 1 is a schematic of a laser cavity configuration with a plano-plano resonator. A 120mm length laser rod in 4mm diameter is considered in the simulations. The flat mirrors M_1 and M_2 are located at a distance of L_1 and L_2 from the principal plane of the laser rod, respectively. The mode radius ω_0 at the principal plane can be calculated by the Magni method. It increases to infinity as the cavity works at the limits of the stability zones for radial polarization (TM mode) or azimuthal polarization (TE mode). Using the stability criterion, the refractive power D at the stability limit can be obtained

$$D = \begin{cases} 0 \\ \dfrac{1}{L_1} \\ \dfrac{1}{L_2} \\ \dfrac{1}{L_1} + \dfrac{1}{L_2} \end{cases} . \quad \left(\text{Assume} L_1 > L_2\right) \quad (8)$$

Figure 2(a) and 2(b) show the theoretical mode radius without and with laser cooling under consideration for L_1 = 833mm, L_2 = 463mm, R = 90%, respectively. The pump power lower than the threshold P_{th} is omitted in Fig. 2(b). In a real system, the existence of the internal power reduces the refractive power of the thermal lens. This effect of laser cooling on the radial and azimuthal polarization stability zones is clearly shown in Fig. 2. We can see that the stable zones of the TE and TM modes move to right when laser cooling takes into account. Furthermore, due to the diminution of the thermal load parameter (χ_{eff} is less than χ), the TE and TM modes stable regions, as well as the overlap zone between them, are enlarged.

In Fig. 2 (c) and 2 (d) the theoretical refractive power and the output power of the working cavity versus the pump power are shown. Firstly, pay attention to the process of increasing the

#151807 - $15.00 USD Received 27 Jul 2011; revised 20 Aug 2011; accepted 22 Aug 2011; published 2 Sep 2011

pump power (loading process). After the pump power exceeds the threshold point P_{th}, the laser operates in the overlap zones (region from the threshold point P_{th} to point a) of the TE and TM stability zones with multimode output. In region ab, the laser works in a TE_{01} single mode. It is one of the two zones to achieve a TE_{01} mode beam. Another zone to obtain a TE_{01} mode beam is the region gh. At point a, the output power drops slightly due to the laser mode variation from the multimode to the TE_{01} mode. Meanwhile, the refractive power rises because of the reduction of the internal power. As the laser crossing point b, the right limit of the TE mode stable zone, the output power falls sharply and the lasing ceases. The output power is zero and the refractive power increases with the pump power in region bc. When the resonator travels through region cd, interesting phenomena appear. At point c, the laser does not restart and the refractive power of the TM mode D_r reaches $1/L_2$, which is the limit of the stable zone described in Eq. (8). Then the increased pump power tends to drive the laser into the TM stable state and lases with a TM_{01} mode beam (as shown in Fig. 2(a)). However, the increased internal power tends to decrease the D_r and drive the resonator back into the unstable state. Then periodic oscillation of the output power appears [17], and the D_r is confined around $1/L_2$ (Fig. 2(c), region cd), locking the laser close to the stability limit in a dynamic equilibrium. Zone ef is a similar region with zone cd, except that the TM mode beam always exits. At point e, D_φ reaches $1/L_2$ and the TE mode presents with the internal power increasing slightly. However, the increased internal power drives the TE mode back to the unstable zone. Then, the output power oscillation and the transverse mode hopping appear.

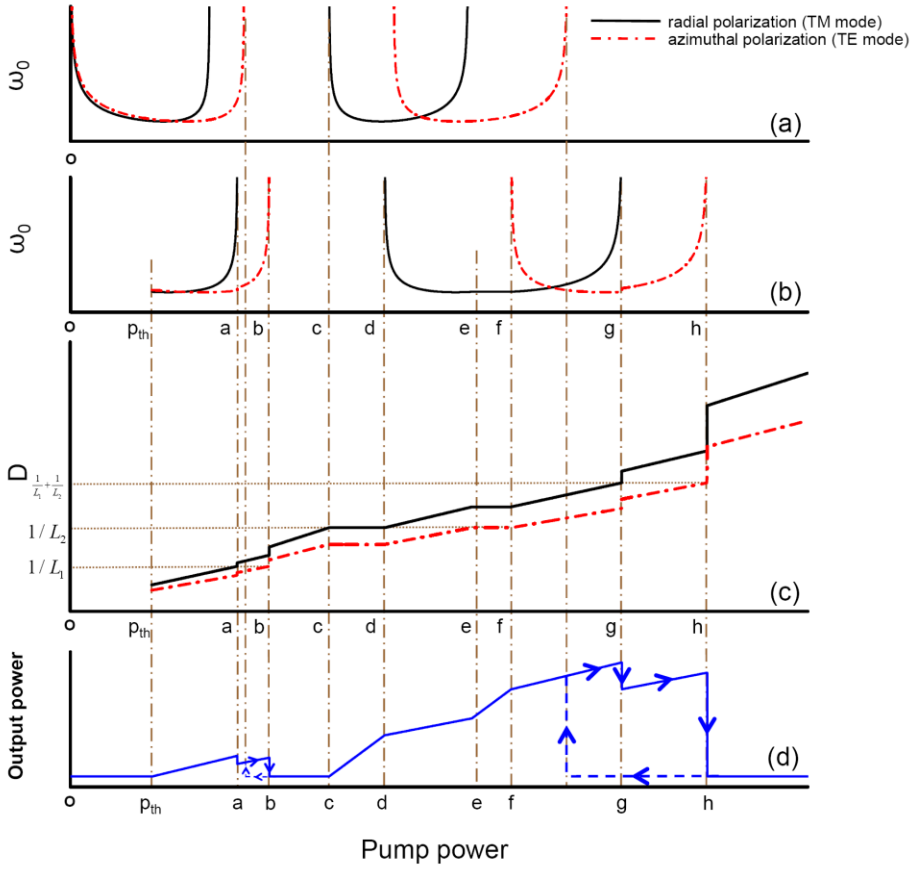

Fig. 2. Simulation of the laser performance with and without laser cooling taken into account: (a) Stable zones without lasing. (b) Stable zones for a working cavity. (c) Refractive power versus pump power in the loading process. (d) Output power versus pump power in the loading (solid line) and unloading (dash line) processes.

#151807 - $15.00 USD Received 27 Jul 2011; revised 20 Aug 2011; accepted 22 Aug 2011; published 2 Sep 2011

This special region may be unconspicuous or even disappears when the additional TE mode light does not provide a large enough internal power increment. As described above, a laser operating in region cd lases in the TM_{01} mode but with the output power unsteady, while in region ef, the output power is unsteady and the mode is mutable. These two special regions surround an optimum region to achieve TM_{01} mode (region de). The region de is the appropriate region to produce a TM_{01} single-mode beam without huge output power fluctuation or mode variation. Therefore, we suggest that it is better to produce steady TM_{01} mode beams in the region de. At point f, the output power increases linearly until it reaches the radial polarization critical point g and the power falls off (Fig. 2(d), region fg). The laser continues to run at a reduced power until the azimuthal polarization becomes unstable and the laser shuts off. As the plot shows, in region gh a high-power TM_{01} mode beam can be obtained with a high pump power.

Compared with the loading process, the laser performance is slightly different in the process of decreasing the pump power (unloading process). Due to the absence of laser cooling, the laser oscillation does not restart at point h or point b in Fig. 2 (b) when decreasing the pump power from the unstable zones. Instead, the laser oscillation restarts at lower pump power, which corresponds to the limit of the TE mode stable zones under the non-lasing condition in Fig. 2 (a). Therefore, thermal hysteresis loops appear around the right edges of the stable zones through the loading and unloading processes as shown in Fig. 2(d). When the laser is operating inside the regions of the thermal hysteresis loops and suffering from a large power fluctuation, laser oscillation may be interrupted and cannot restart again. Unfortunately, thermal hysteresis loop regions always have overlap zones with the regions to produce TM_{01} mode beams as shown in Fig. 2. Therefore, the large power fluctuation should be avoided when producing TM_{01} mode beams. In region gh, with higher pump power than region ab, a high-power TM_{01} mode beam can be obtained. However, when the laser is operating near point h, the output power becomes unsteady and large power fluctuation may occur. Thus, it is suggested to produce high-power and steady TM_{01} mode beams in region gh but away from point h.

4. Experiments

Based on the analysis in section 3, we experimentally demonstrate the generation of radially and azimuthally polarized laser beams with a Nd:YAG laser. The experiment configuration is the same as shown in Fig. 1. The flat mirror M_1 with 90% reflectivity at 1064nm is used as an output coupler. Another flat mirror M_2 is a high-reflectivity rear mirror. A commercial laser diodes side-pumped Nd:YAG module is installed in the cavity. The Nd:YAG laser rod is 4mm in diameter and 120mm in length. The maximum pump power of the module is about 500W at the driven current of 24A, and the threshold current of the pumping laser diodes is 8A. The output power of the beam is measured by a power meter. Profiles of the entire beams and those after passing through a linear polarizer are captured by a CCD.

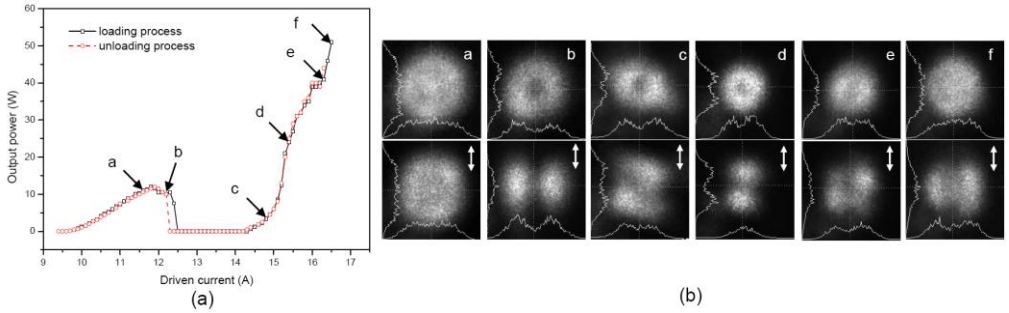

Fig. 3. Laser performance in the experiment with a cavity configuration for L_1 = 833mm and L_2 = 463mm: (a) Output power versus driven current in the loading (solid line) and unloading (dash line) processes, (b) Profiles of the beams that before (upper) and after (lower) passing through a polarizer.

#151807 - $15.00 USD Received 27 Jul 2011; revised 20 Aug 2011; accepted 22 Aug 2011; published 2 Sep 2011

Firstly, a resonator with L_1 = 833mm and L_2 = 463mm is configured. Experiment results are shown in Fig. 3. As seen in Fig. 3(a), a thermal hysteresis loop is presented around the driven current of 12.4A. Besides the thermal hysteresis loop, the laser performance is the same in the loading process and the unloading process. Before the output power drops slightly at I = 11.9A, the laser is working in a multimode at I = 11.6A with a Gaussian beam profile shown in subgraph (a) of Fig. 3(b). The upper and the lower graphs with cross-sections of major axes show the profiles of the beams that before and after passing through a linear polarizer. The white arrowhead on the subgraph shows the polarization direction of the polarizer. After the slightly drop point, the beam profile of the restarting point at I = 12.2A is shown in subgraph (b). It exhibits a TE_{01} mode with a purity of 83% (the ratio of the power with pure radial or azimuthal polarization to the total beam power). Note that, at this moment, the laser is operating out of the thermal hysteresis loop and lasing with a 10 W steady TE_{01} mode beam. The output power instability is about 8% in an hour. Through the unstable zone from I = 12.5A to 14.4A, laser oscillation appears again at I = 14.4A. The intensity distribution at I = 14.8A is shown in subgraph (c). At this point, the laser is working inside the special region (region cd) as described in section 3. The output power swings regularly. However, the intensity distribution, which is of a ring shape like a TM_{01} mode, remains the same during the output power fluctuation. When the driven current increases to 15.4A, a 25 W TM_{01} mode beam with the purity of 79% and the instability of about 12% is obtained as seen in subgraph (d). At this moment, the laser is working in the appropriate place for generating TM_{01} mode beams. As the driven current continues growing, the beam mode becomes mutable. Subgraph (e) is one of the beam profiles in this region at I = 16.3A with the intensity distribution varying among the petal shape, Gaussian shape and ring shape. It means that the TE mode has appeared, but been unsteady. In addition, it is interesting to find that the output power is comparatively steady. At last, the driven current is set to 16.5A. The beam profile becomes Gaussian shape as seen in subgraph (f) and the output power is measured to be 50 W. The intensity distribution of the beam after passing through a polarizer shows that azimuthal polarization is dominant, but it still seems close to the multimode beam. In case of the laser rod overheating, the driven current cannot be increased over I = 16.5A in this cavity configuration.

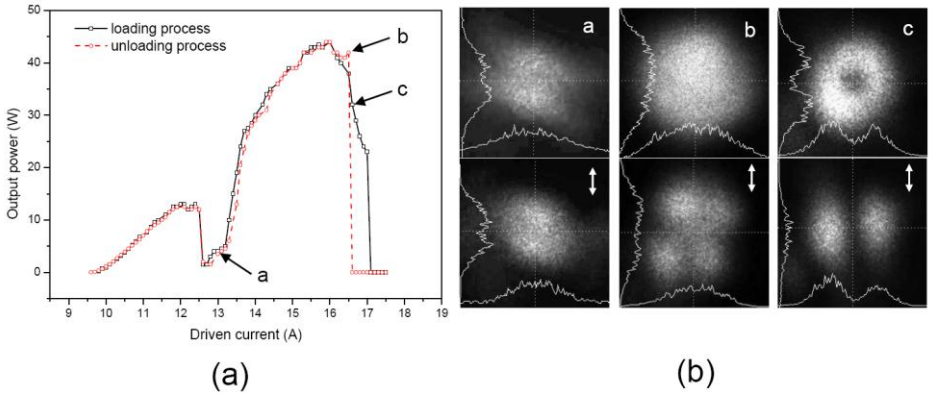

Fig. 4. Laser performance with a cavity configuration for L_1 = 833mm and L_2 = 633mm: (a) Output power versus driven current in the loading (solid line) and unloading (dash line) processes, (b) Profiles of the beams that before (upper) and after (lower) passing through a polarizer.

Secondly, the resonator is reconfigured with L_1 = 833mm and L_2 = 633mm. The same experiment is performed and the results are exhibited in Fig. 4. It is shown that the performance is a bit different from previous experiment. Both of the two stable zones are observed at this time, but they are not separated clearly. In the previous experiment, the stable zones are the same as the simulation that shown in Fig. 2(b) with point b locating on the left of point c. The lasing ceases in region cd. However, in this experiment, the two stable zones

#151807 - $15.00 USD Received 27 Jul 2011; revised 20 Aug 2011; accepted 22 Aug 2011; published 2 Sep 2011

get closer due to the reconfiguration of the resonator. Point b is locating on the right of point c now. It means that the unstable region cd disappears. Subgraph (a) of Fig. 4(b) shows the intensity distribution of the laser beam in the hollow region at I = 13A. Here, the laser is lasing in a multimode. The thermal hysteresis loop, which should appear around the right edges of the first stable zone, is absent due to the disappearance of the unstable region cd, substituted by a hollow region with the lasing around I = 13A. Furthermore, another thermal hysteresis loop is present from I = 16.5A to 17.0A. Subgraph (b) illuminates the beam profile at the restarting point I = 16.5A. The multimode distribution suggests that the laser is operating in the overlap zone as described in section 3 in region fg. For obtaining a TE_{01} mode beam, the driven current should be increased above 16.6A. Then the operating point is inside the thermal hysteresis loop and a 32 W stable TE_{01} mode laser beam with the purity of 80% and the instability of less than 9% is obtained. The beam profiles are shown in subgraph (c). The oscillating interruption should be considered at this moment.

5. Conclusion

A modified thermal model of a working cavity is used to analyze the laser resonator with a uniformly pumped isotropic solid-state rod. The model shows a reduction of the thermal load under the lasing condition, which is of internal power dependence. Thus, the refractive power of the thermal lensing, which is caused by the thermal heat dissipating in the laser rod, is variable not only with the pump power but also with the internal power of the cavity. According to this thermal model and combining with the Magni method on the cavity analysis, we calculate the stable zones of the TE and TM modes of a working cavity. The simulations show that both of the radial and azimuthal polarization stable zones shift to the higher pump power side. Also, the characteristics of the cavity in the loading and unloading processes are theoretically analyzed in details. The output power performance and the polarization behavior are studied experimentally through a Nd:YAG laser. The experiment results match well with the theory predictions. High-power and steady TE_{01} and TM_{01} modes beams are obtained in the experiments. And both of the simulations and experiments show that special regions and thermal hysteresis loops are present around the edges of the stable zones.

Acknowledgments

The work was partially supported by the National Natural Science Foundation of China under Grants No.10732100, 11072271, 10972239, 61008025 and the Specialized Research Foundation for the Doctoral Program of Chinese Higher Education under Grant No.20100171120024 and the Fundamental Research Funds for the Central Universities of China under Grant No. 11lgpy55.

#151807 - $15.00 USD Received 27 Jul 2011; revised 20 Aug 2011; accepted 22 Aug 2011; published 2 Sep 2011